SIMULATION OF DIFFUSION IN HETEROGENEOUS MEDIA

by

Paul Ionele

A dissertation submitted to the University of Ontario Institute of Technology in accordance with the requirements of the degree of Bachelor of Science (Hons) in the Faculty of Science.

March 20, 2016

UNIVERSITY OF ONTARIO
INSTITUTE OF TECHNOLOGY

ABSTRACT

This is a short example of an abstract.

ACKNOWLEDGEMENTS

Thank some people that you like here.

AUTHOR'S DECLARATION

I declare that the work in this thesis was carried out in accordance with the regulations of the University of Ontario Institute of Technology. The work is original except where indicated by special reference in the text and no part of the dissertation has been submitted for any other degree. Any views expressed in the dissertation are those of the author and in no way represent those of the University of Ontario Institute of Technology. The thesis has not been presented to any other University for examination either in Canada or elsewhere.

Paul Ionele
March 20, 2016

Contents

1. INTRODUCTION

What was/is the purpose of this thesis? Why did we develop these computational simulations? Really, we need a goal!

We begin with an overview of basic theory on: diffusion, Monte Carlo methods, and master equation methods.

1.1 Diffusion Theory

Diffusion is a natural phenomenon caused by the tendency of small particles to spread out, or diffuse, in a given space. In a solution and at the microscopic level, the motion of particles is driven by thermal effects and particles collide in a practically random manner. If one was to track an individual particle, they would find its path to be chaotic—a 'random walk'. As we will see, the random motion of individual particles can be modelled as a Monte Carlo random walk and the overall motion of many particles can be treated using a probabilistic approach using master equations.

insert random walk figure here

Observing the solution from a macroscopic level, it appears that these collisions result in the movement of particles from an area of high concentration to an area of low concentration. The process is observable until the system has reached a particle concentration equilibrium. This equilibrium is a dynamic state, not a static one; overall diffusion may have stopped, but particles continue to move. Even with the introduction of semi-permeable boundaries separating a high particle concentration region from a low concentration region, if the particle is able to permeate the bound-

ary, an equilibrium can still occur because particle flux across the boundary is equal in opposite directions.

In the simple cell models developed and analyzed, the region in which particles may exist is heterogeneous since it is divided by semi-permeable boundaries and each boundary encloses a region of different diffusivity. The diffusion process still occurs, but particle motion is mediated by the absolute reflecting boundaries of the system and more importantly, by the semi-permeable boundaries. The semi-permeable boundaries behave in a passive transport manner and are considered to facilitate the process of simple diffusion. The boundary conditions necessary to simulate passive transport and required to reach an equal concentration equilibrium are explained later.

In order to perform an analysis of diffusion behaviour in the simple cell models, a measure for the extent of particle motion was necessary. In the case of undirected motion, the time-average particle position $\langle x \rangle$ is not a very useful quantity. Although the particle moves randomly, the expectation value for the position is equal to its starting position x_0. The time-average position-squared $\langle \Delta x^2 \rangle$, also known as the mean-squared-displacement (MSD), is not equal to x_0. The MSD may be computed if individual particle positions are known or if the particle density distribution is known at some time t_n. Let x_i be the position of the i$^{\text{th}}$ particle at t_n, the MSD is:

$$\langle \Delta x^2 \rangle = \langle x_i^2 \rangle + \langle x_i \rangle^2 \tag{1.1}$$

The MSD calculated at each time step can be used to derive other quantities of interest such as the effective diffusivity constant D_{eff} at any point in time. Albert Einstein related the macroscopic diffusivity constant to the microscopic random walk via the MSD (J. Philibert , 2006).

$$\langle \Delta x^2 \rangle = 2Dt \cdot d \tag{1.2}$$

Where D is the diffusion coefficient and d is the dimensionality of the system ($d = 1$ was used for all calculations since we were interested only in the MSD in one direction). Solving for the effective diffusivity:

$$D_{\text{eff}} = \frac{\langle \Delta x^2 \rangle}{2t} \tag{1.3}$$

Einstein's diffusion equation as we may call it, says that the MSD scales linearly in time. While this is true for *steady diffusion*, this is not always true for systems where *anomalous diffusion* occurs. For a system undergoing a steady diffusion process, the log-log plot of MSD versus time has a slope of unity, since t is raised to the power of 1 in Equation 1.2. For most systems studied, there was some non-linearity in time indicating the presence of anomalous diffusion.

insert anomalous diffusion figure

We introduce a modified Einstein's diffusion equation with an additional exponential factor β, to calculate a quantity $\beta(t)$ that is useful for characterizing the kind and magnitude of the anomalous diffusion process at any time.

$$\langle \Delta x^2 \rangle = 2D \cdot t^{\beta} \tag{1.4}$$

Taking the base-10 logarithm of both sides of Equation 1.4:

$$\log\left(\langle \Delta x^2 \rangle\right) = \beta \cdot \log(t) + \log(2D) \tag{1.5}$$

On a linear plot, this appears as a relation of the form $Y = \beta X + C$ and if $\beta = 1$, then the diffusion process is steady. It is possible to determine what β is as a function of time. If we take the derivative dY/dX, then:

$$\frac{dY}{dX} = \beta(t) \tag{1.6}$$

A plot of $\beta(t)$ versus t reveals the magnitude of the non-linearity and identifies if the diffusion process occurring sub- or super-diffusive at a particular time. For a sub-diffusive process $\beta < 1$, for a super-diffusive process $\beta > 1$, and for steady diffusion $\beta = 1$.

$$D_{\text{eff}} = \frac{\langle \Delta x^2 \rangle}{2t} \tag{1.7}$$

Plots of D_{eff} and β versus $\log(t)$ may be constructed and are useful in determining how the long-time effective diffusivity depends on the semi-permeable boundary transition probability, ratio of cellular to extracellular diffusivities, and system geometry.

1.2 Monte Carlo Theory

Introduction. Theory. Supporting figures.

1.3 Master Equation Theory

With an enormous number of particles, all randomness disappears and it looks as though the particles move smoothly and deterministically from areas of high concentration to low concentration.

1.4 Simple Cells and Tissues

Nearly all human cells are microscopic in size; their diameters range from 7.5 µm to approximately 150 µm and a cell exhibits a particular size or shape that reflects the specific task it's designated to perform. There are many different types of cells including nerve cells, muscle cells, and gland cells, but despite their anatomical and functional differences, the cells of the human body have many similarities. It is a fact

that no cell contains all cellular components found in all the cell types, so often a composite cell (Figure 1.1) is used to exhibit the most important characteristics.

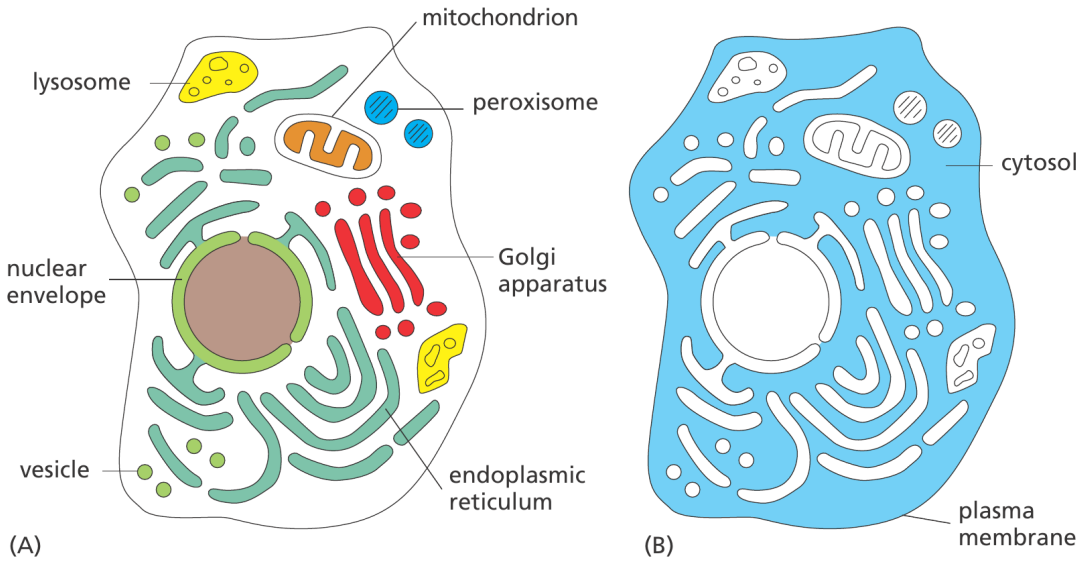

Figure 1.1: Composite cell showing various important and common internal cell structures. Most of the volume within the cell is occupied by the cytosol fluid. Figure courtesy of Essential Cell Biology, Alberts, 3rd.

Each cell is enclosed by a plasma membrane that separates the cell contents from the surrounding environment. The inside of the cell is mostly composed of a gel-like substance called cytoplasm that is a dense arrangement of proteins, organelles, and other molecules, suspended in a watery fluid called cytosol. The dense crowding of molecules and organelles results in frequent physical interactions which promotes high metabolic efficiency (Patton, Thibodeau , 2013). All of the fluid inside the cell may be referred to as intracellular fluid or simply, cellular fluid (CF).

The CF is separated from the extracellular fluid (ECF) by the cell/plasma membrane. This membrane is a phospholipid bilayer with various embedded macromolecular structures. Each phospholipid molecule is amphiphatic, having both a hydrophobic and hydrophilic region. A collection of phospholipid molecules will naturally arrange themselves into a bilayer that does not allow water, polar molecules, or ions to pass through easily. However, water and other molecules or ions need to traverse this

membrane and the water transporting task is accomplished by aquaporin gated channel proteins. Aquaporins facilitate the passive diffusion of water through the plasma membrane, between the intracellular and extracellular regions. (Patton, Thibodeau , 2013).

1.4.1 Tissues

In a multicellular organism, there are several levels of biological organization. A cell is the lowest level of organization that is considered living; tissues are the next higher level of organization and are composed of cells similar in structure and function. This ensemble of cells resides in an extracellular matrix (ECM); a medium containing water, fibrous and adhesive proteins, glycoproteins, and other molecules. The ECM varies in composition between different tissues, but providing structural support and facilitating cell-to-cell communication are common functions of the ECM. In some cells, the cytoplasm is more viscous than the extracellular matrix (Campbell, Reece , 2008). At the cellular level some tissues are relatively organized.

In this project, a simple tissue model was constructed based on some basic defining characteristics of real cells and tissues. The simple tissue model consisted homogeneous spaces, specifically more viscous intracellular regions and less viscous extracellular regions separated by a passive semi-permeable boundary. All of the cells in a model were of the same dimensions and repeated in series.

2. MODELS AND SIMULATIONS

A simulation is intended to imitate in many cases, a real-world process or system that may be too difficult or costly to analyze directly. Before any such simulation can begin, a model of the system studied must be constructed. Models capture the characteristics and behaviours of the system they represent and in general, a model should be as simple as possible (since resources are limited) while still explaining experimental observations and making predictions with a given degree of accuracy. The simulation is the implementation of the model and can be executed on a computer to produce data for testing, analysis, and visual presentation.

In our simplified model of a biological tissue, the relatively ordered and periodic nature of cells in some simple tissues is captured as a series of repeating *unit cells*. These unit cells are the building blocks of the heterogeneous 1D and 2D models explored in this project. Each unit cell is characterized by a cellular domain, separated from an extracellular domain by a semi-permeable membrane/boundary. The domains are isotropic except at the boundaries where a change in diffusivity (diffusion coefficient) and semi-permeable boundary exist. Within each domain, the only characteristic modelled is the diffusivity of ideal particles, and is implemented as a directional stepping probability (Section 1.1). For all of the models, the cellular domains had smaller diffusivities than the extracellular domains, similar to some real tissues. Regarding the boundaries, there exists+ two kinds in our models. The first kind is a totally-reflecting boundary; it forms the absolute boundary of the model system and represents an insurmountable physical boundary. The second kind is a

semi-permeable non-active/passive boundary and represents the selectively permeable nature of the plasma membrane. In a real biological plasma membrane, the integral membrane-bound proteins can facilitate either active or passive transport. In the simple cell model developed, the semi-permeable membranes behave in a passive transport manner and this is implemented as a boundary transition probability, a concept explained in Section 1.1.

The simulations executed and subsequently analyzed were that of particle diffusion. More specifically, the diffusion of idealized, non-interacting particles experiencing zero net force, and adhering to boundary constraints. Particle motion was therefore undirected but occurred in only one direction (along a line) in the 1D system, and in two orthogonal directions in the 2D system. For each time step, each particle was allowed to move in only one direction or stay in its current location and since particles were non-interacting, multiple occupancy of lattice sites was permitted.

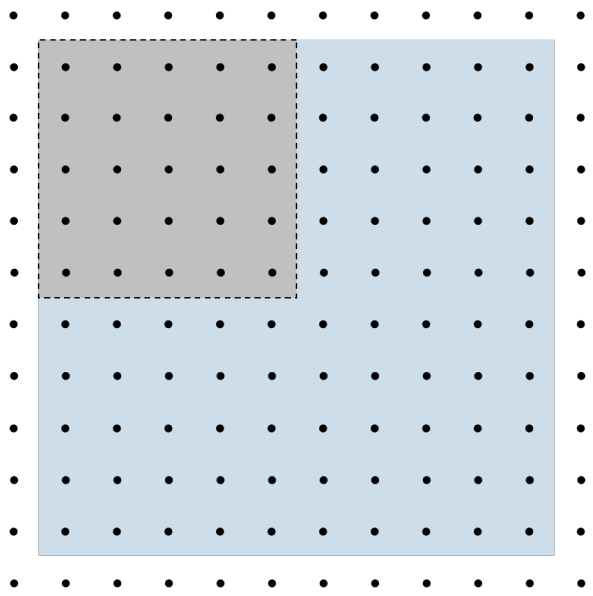

Figure 2.1: A single 2D unit cell forms the building block of the 2D model. An example lattice arrangement is overlayed on the model to show possible particle positions. The dimensions of each domain can be adjusted individually by changing the number of lattice sites used to define each dimension. Dashed lines represent semi-permeable boundaries and lattice sites (dots) outside the cell belong to adjacent cells.

It was decided from the start of the project that particles would move in the system

by a constant jump/step-size, compared to a continuum step-size (ex. Gaussian). Although this particle behaviour is generally less representative of a real diffusion process and less accurate compared to continuum Monte Carlo (MC) methods and molecular dynamics simulations, the data generated would still be sufficiently accurate for our analytical purposes and be faster to compute. Fixed step-sizes in the particle movement results in a grid or lattice-like arrangement of particle positions over time. The process simulated is therefore said to be occur on a lattice as the particles are free to move, but only to fixed lattice positions. This manner of particle movement was implemented in both the MC and master equation (ME) simulations.

Overall, the goals were to simulate the process of diffusion for homogenous and heterogeneous systems using MC and ME methods, calculate a mean-square-displacement (MSD) for every time step from the computed density distribution, and from the MSD, determine an effective diffusivity for the system at any point in time. For both the MC and ME simulations, the particle density distribution data output was of the same form. MSD calculation implementations varied slightly between the MC and ME simulations, but the calculations for effective diffusivity were the same.

2.1 Monte Carlo Simulations

Using MC-based algorithms, information on the individual state of each particle including current position and path history, can be maintained. However, due to the finite number of particles used in the simulation and the stochastic nature of individual particle motion, statistical fluctuations lead to 'non-smooth' density distributions. The use of MC algorithms in simulating the process of diffusion was motivated by the random nature of the diffusion process (Section 1.1) at the level of the individual particle.

2.1.1 1D Homogenous and Heterogeneous Systems

A natural starting point for the project was 1D systems since they are more simple to model and simulate/program than those which are multidimensional. In our 1D simulations, particles move along a line and at any given lattice site, can move to either one of the two neighbour sites, unless an absolute boundary is met. A particle step-size of one lattice unit was used, meaning that a particle stepped only a single lattice site in a randomly selected direction, each time step. This stepping distance is currently uncorrelated/uncalibrated with any physical or real distance. Each time step in the simulation is also uncorrelated with any characteristic or real time; in the simulation it is simply an integer used as a loop variable. Length and time-scale correlation with physical systems is possible but such an endeavour is outside the time limits of the current project.

In the homogenous system (Figure 2.2) where particle motion is unbiased, a particle that is not at the absolute lattice limits has an equal probability to step one lattice unit in either direction (we'll use the x-direction). Let those probabilities be: P_x^+ and P_x^-. The unbiased particle motion requirement is met by ensuring $P_x^+ = P_x^-$. We can introduce another physically sensible probability; the probability that a particle does not move in a given time step. Let this probability that a particle stays at its current lattice site for the time step be: $P_x^s = 1 - P_x^+ - P_x^-$. If not at an absolute boundary, the particle has three possible future states. At the absolute boundaries, the particle has only two possible future states; it may move from its current lattice site in a direction away from the boundary, or it may stay at its current lattice site. For example, with reference to Figure 2.2, if the particle is at the leftmost boundary, then it can only move to the right neighbour lattice site or stay at its current lattice site. Therefore the probabilities for the particle's motion depend on its position within the system and for this example they are: $0 < P_x^+ \leq 1$ and $P_x^s = 1 - P_x^+$. It should be noted that reflecting boundaries in the simulation model a situation where a particle attempts to

move through the boundary, but is 'reflected' back to its starting position. Therefore, in the simulations, the probability of moving towards the boundary is not zero, it is the probability of crossing the boundary that is zero. Since the events of moving towards the boundary and crossing the boundary are treated as mutually exclusive, the total probability of a particle transition into a different domain is the product of the two individual probabilities. In the simulations, the position of the particle within the system is determined and P_x^s and $P_x^{-,+}$ are automatically appropriately set. At this point, it may be interesting to ask "What if the transition probability is not zero at the absolute boundaries?". If the computer simulation does not break from accessing memory space outside a predefined array, then one obtains the case for a semi-permeable boundary and this will be detailed later on.

Figure 2.2: Homogenous 1D cell model with lattice overlay. The sold lines represent the absolute physical limits of the system and behave as reflecting boundaries.

In the heterogeneous system (Figure 2.3), a particle that is not at the absolute lattice limits and is not at a lattice site next to a semi-permeable boundary, has an equal probability to step one lattice unit in either direction, same as in the homogenous system simulation. Particle behaviour at the absolute boundaries was handled the same way as in the homogenous system. The different diffusivities of the cellular and extracellular regions were simulated by using different stepping probabilities. We introduce the subscripts i and e to differentiate between stepping probabilities in the (*intra*)cellular and extracellular domains: $P_{x,i}^{+,-}$ and $P_{x,e}^{+,-}$. Within each domain and excluding the lattice points at the boundaries, the behaviour of the particles was like that of the homogenous system. At the semi-permeable boundaries, the following condition (Section 1.1) was necessary if the long-time density distribution was to be

physically reasonable:

$$P_{\mathrm{e}\to\mathrm{i}} = \left(\frac{P_{x,\mathrm{i}}}{P_{x,\mathrm{e}}}\right) P_{\mathrm{i}\to e} \tag{2.1}$$

This equation relates the boundary transition probabilities $P_{e\to i}$ (extracellular to cellular transition) and $P_{i\to e}$ (cellular to extracellular transition) between regions of different diffusivities, characterized by the directional stepping probabilities $P_{x,i}$ and $P_{x,e}$, *under the condition* $P_{x,i} < P_{x,e}$ (Section 1.1). Note that $P_{e\to i}$ *or* $P_{i\to e}$ may be set arbitrarily, but one determines the other according to Equation 2.1; they cannot be set independently if the correct density distribution in the long time is desired.

As an example, consider a particle at a lattice site adjacent to semi-permeable boundary. If the particle is in a cellular region, the total transition probability for the particle to the extracellular region is the product of the transition probability from the cellular to extracellular region and the *cellular* directional stepping probability.

$$P_{\mathrm{total},\,\mathrm{i}\to\mathrm{e}} = \left(\frac{P_{x,\mathrm{e}}}{P_{x,\mathrm{i}}}\right) P_{\mathrm{e}\to i} \cdot P_{x,i} \tag{2.2}$$

Using Equation 2.1 for the transition probabilities, the total transition probability across any semi-permeable boundary can be determined. In the case of absolute reflecting boundaries, the transition probabilities in Equation 2.1 are zero, and hence the total transition probability is zero.

Figure 2.3: Heterogeneous 2D unit cells with cellular and extracellular regions. Dashed lines indicate semi-permeable boundary, separating regions characterized by different diffusivities. Dots outside coloured regions indicate continuity of system.

All directional stepping probabilities, boundary transition probabilities, region dimensions, number of particles used, and time step limit are initialized prior to running the simulation. More specifically, the region dimensions are defined by a number of lattice sites used for that region (i.e. the length of a cellular space could be set as n lattice sites) and the size of a unit cell is the sum of lattice sites in the cellular and extracellular regions. Therefore, the density of lattice sites within any region is always the same, regardless of the size of that region. The total length of the system is the product between the number of lattice sites used in a unit cell and the number of unit cells.

Our MC-based simulations of diffusion require a 'random' number generator. Pseudo-random numbers, drawn from a uniform distribution, were generated during the execution of the simulation using the `rand()` C-library function and `RAND_MAX` built-in constant. It was desired that the random numbers (rnd) be uniformly distributed over the interval $0 \leq \text{rnd} < 1$, so all random numbers returned by the `rand()` call were normalized by `RAND_MAX`.

The simulations produced a particle density distribution at every time step. One of the goals of this project was to compute the MSD of the particles at every time step and collect this data for further analysis. Since the individual position of each particle was tracked during the simulation, it was possible to calculate the MSD of all particles for a time t_n. Let x_i be the position of the i$^{\text{th}}$ particle at t_n, the MSD is:

$$\langle \Delta x^2 \rangle = \langle x_i^2 \rangle + \langle x_i \rangle^2 \tag{2.3}$$

The angle brackets indicates the sum of the positions divided by the number of particles:

$$\langle x_i^2 \rangle = \frac{1}{N} \sum_{i=1}^{N} x_i^2 \tag{2.4}$$

$$\langle x_i \rangle = \frac{1}{N} \sum_{i=1}^{N} x_i \tag{2.5}$$

Since the particles experienced no external force, it was expected and shown that for every time step, $\langle x_i \rangle \approx x_0$, where x_0 is the position/index of the initial starting lattice site of all the particles. The mean-squared-position $\langle x_i^2 \rangle$ was not constant for every time step, it increased with time reflecting the 'spreading' of the particles outwards from their origin.

The output of our simulations was two *.txt files. One file contained the density distribution data computed at every time step. The second file contained the simulation analytics: $\langle x_i \rangle$, $\langle x_i^2 \rangle$, and MSD data computed from the density distribution for every time step. These quantities were all that was needed for further calculations and the creation of various plots for analysis purposes. From the MSD, effective particle diffusivities could be computed for various cellular and extracellular diffusivities, semi-permeable boundary transition probabilities, and geometrical variations of the model. The density distribution data was processed by a separate program to create plots for every time step; the result an animation of the particle diffusion process in the system.

2.1.2 2D Heterogeneous Systems

Simulations of particle diffusion were also performed for 2D systems. The 2D model developed and simulated was heterogeneous; no homogenous model was developed. The MC algorithm for the simulation of the 2D system was in principle the same as for the 1D heterogeneous system, however, there are a few important differences to note. For every given time step, a particle at some lattice site that is not at an absolute boundary has four directional steps available and particle movement in the orthogonal directions are independent but cannot both occur in a single time step.

Similar to the 1D simulation, the 2D unit cell is the building block of the 2D model, the particle moves 'on a lattice', and a step-size of one lattice unit is permitted. Each unit cell consists a cellular region separated from an extracellular region by a semi-permeable boundary. A key characteristic of the unit cell is that, when linked in series, an extracellular channel is formed providing particles the option to move freely without obstruction. In Figure 2.4, this is visible as an uninterrupted region or channel in the lower half of the figure. It is possible to arrange more than one series of unit cells so that a larger $(m \times n)$ unit cell configuration is obtained, but this was not studied. Only $(1 \times n)$ unit cell models were simulated.

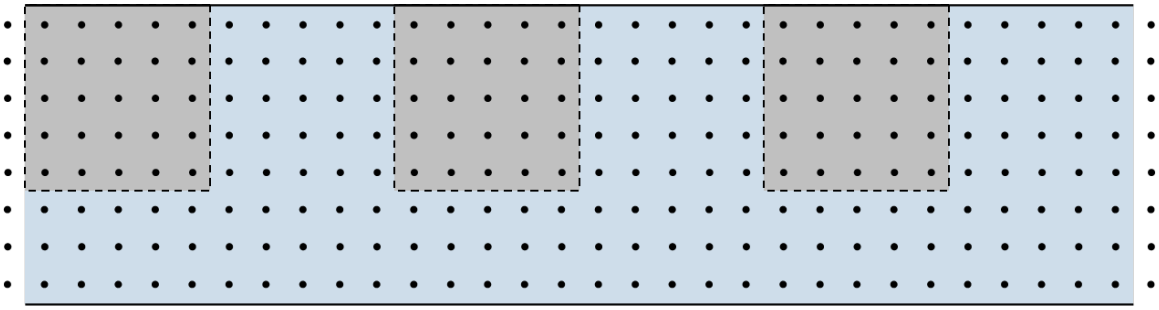

Figure 2.4: A $(1 \times n)$ series configuration of 2D unit cells with cellular and extracellular regions. Dashed lines indicate semi-permeable boundary and solid lines indicate absolute boundary. Dots outside the coloured region indicate continuity of the system.

In 2D, there are an additional two neighbour lattice sites the particle can move to. If not at an absolute boundary, the particle has five possible future states. At the absolute boundaries, the particle has only 4 possible future states; it may move from its current lattice site in a direction away from the boundary, along the boundary, or it may stay at its current lattice site. We introduce an additional set of directional stepping probabilities in $\hat{y}$: $P_{y,i}^{+,-}$ and $P_{y,e}^{+,-}$. The directional stepping probabilities in $\hat{x}$ and $\hat{y}$ have the conditions: $0 < P_{i,e}^{+,-} \leq 0.25$. For unbiased motion (excluding boundary lattice sites) all directional stepping probabilities must be equal. Therefore, the probability that the particle y-coordinate does not change for a given time step is $P_y^s = 1 - P_y^+ - P_y^-$. Similarly for the x-coordinate $P_x^s = 1 - P_x^+ - P_x^-$. So the total

probability that a particle remains at its current lattice site is $P^s = 1 - P^s_x - P^s_y$. When a random number is generated, its value is tested for membership in intervals defined by the stepping probabilities, and this determines the motion of the particle.

Handling of the boundary transition probabilities was done in the same manner as the 1D simulation, in accordance with Equation 2.1. In the program developed, for every time step, the current particle position and possible future particle position are compared. If it is found that the future possible position is in a different region than the current position, then the probability to cross into the new region is automatically set using Equation 2.2 solved for $P_{\text{total, i}\to\text{e}}$ or $P_{\text{total, e}\to\text{i}}$. Absolute boundaries were implemented as reflecting boundaries.

Similar to the 1D simulations, density distribution data and other analytical data was computed and written to *.txt files. The density distribution data output was in a matrix form; each line of data represented a different row of lattice sites in the system. For each time step, all rows were written to the file and an empty line inserted before writing data for the next time step, for parsing purposes. Producing 2D animations of the diffusion process required a program different than the one used to create the 1D animations; however, similar programs were used to simulation analytics.

2.2 Master Equation Simulations

Using the ME methods and evolving the particle density distribution in time, discontinuities in the distributions due to statistical fluctuations are no longer an issue; however, at the expense of information on individual particle state. Using this method, it is not possible to know individual particle position history which restricts the use of certain analyses. For example, it is not possible to reconstruct the paths of particles through the system which can be used to generate a frequency histogram to score the number of times a particle crosses a semi-permeable boundary. The main reason

for use of the ME methods was that most of our intended analysis only required knowledge of $\langle x_i \rangle$, $\langle x_i^2 \rangle$, and MSD. These quantities could be calculated, although in a slightly different way than implemented in the MC methods. In addition, for the basic models simulated, ME-based simulations were much faster than MC-based simulations. ME simulations were also performed on a lattice and within cellular or extracellular regions, directional stepping probabilities were equal for unbiased motion.

Consider the situation of a single particle at a lattice site that, at a given time step, has a directional stepping probability of $P_x^{+,-} = 0.5$ (similar to a coin-toss experiment). In the MC simulations, a random number is drawn from uniform distribution and tested for membership in the intervals defined by the directional stepping probabilities.

$$\begin{cases} x_0 - 1 & P_x^- : 0.0 \leq \text{rnd} < 0.5 \\ x_0 + 1 & P_x^+ : 0.5 \leq \text{rnd} < 1.0 \end{cases}$$

For a small, even number N of particles, it may not be reasonable to expect that the number of particles that step -1 or $+1$ in $\hat{x}$ is exactly N/2. In terms of particle positions, even though the particles have an equal probability of stepping in either direction, the mean position of the particles $\langle x \rangle$ will likely not equal x_0, the expected value of the mean position. However, the law of large numbers guarantees that the arithmetic mean of the position of the particles practically converges to the expected value in the limit of very many particles. In the ME simulations, it is assumed that there are very many particles, enough that the fluctuation in the mean position of the particles is also assumed zero. Instead of starting with some number of particles at x_0, we start with a particle density ρ_0 at x_0 and evolve the particle density distribution in time.

At absolute and semi-permeable boundaries, the density distribution was, in prin-

ciple, treated similar to how individual particles were treated in MC. Instead of the value of a random number determining the movement of a particle, the evolution of the density distribution to the next time step depended on the probability distribution of possible particle movements at that lattice site. Clarifying with an example, consider a lattice site with particle density ρ_0 in a cellular region and adjacent $(-\hat{x})$ to the site is a semi-permeable boundary. The boundary transition probability follows Equation 2.1 solved for $P_{i\to e}$ and the total transition is probability is:

$$P_{\text{total, i}\to\text{e}} = \left(\frac{P_{x,\text{e}}}{P_{x,\text{i}}}\right) P_{\text{e}\to i} \cdot P_{x,i} \tag{2.6}$$

Therefore, the density distribution at the next time step is:

$$\begin{cases} \rho(x_0 - 1) = \rho_0(x_0) \cdot P_{\text{total, i}\to\text{e}} \\ \rho(x_0 + 1) = \rho_0(x_0) \cdot P_{x,i} \\ \rho(x_0) = 1 - \rho_0(x_0) \cdot P_{\text{total, i}\to\text{e}} - \rho_0(x_0) \cdot P_{x,i} \end{cases}$$

This time-evolution of the density distribution was essentially performed by looping over all lattice sites each time step and at a given lattice site, applying the appropriate directional probabilities (product with the particle density at the corresponding site).

As previously mentioned, the quantities $\langle x_i \rangle$, $\langle x_i^2 \rangle$, and MSD were calculated slightly differently than in the MC simulations, since the position of an individual particle was not known. Known was the density ρ_i at each lattice site i. If the starting density was initialized as $\rho_0 = 1.0$, then at any time step:

$$\langle x_i^2 \rangle = \sum_{i=1}^{N} i \cdot \rho_i \tag{2.7}$$

$$\langle x_i \rangle = \sum_{i=1}^{N} i^2 \cdot \rho_i \tag{2.8}$$

The same programs that were used to create the diffusion process animations and other plots for the 1D and 2D MC simulations, were used for the ME simulations since the output data was the same. Most of the analyses of 2D diffusion were based on ME simulations. At least 1 million time steps were needed to observe various diffusive regimes on an 'infinite' system (30×3030 grid of lattice points was usually enough) and the MC simulations took too much time to test various parameter combinations.

3. RESULTS AND ANALYSIS

In this chapter, we begin an analysis of 1D heterogeneous systems, then move our attention to 2D heterogeneous systems. Although 1D homogeneous systems were simulated, they did not provide any interesting or new insight into diffusive behaviour, therefore those simulations and analytical data are not presented in detail. We begin each section with selected images of simulated density distributions to motivate further analysis. More specifically, we analyze how changing the boundary transition probabilities, region diffusivities, and cell geometry (2D only), affects the mean-squared-displacement (MSD) and show that sub- and super-diffusive regimes exist. Lastly, we show that the long-time effective diffusivity is non-trivial even for simple-cell geometries.

3.1 1D Systems

For very large systems or short simulation times—conditions where the density distribution is zero at the absolute boundaries—agreement between the Monte Carlo (MC) and master equation (ME) simulation solutions, and analytical solutions (3.2) of the 1D diffusion equation with no net drift and constant diffusion factor (3.1), was observed (Figure 3.1).

The 1D diffusion equation 3.1 may be known as a 'simple' Fokker-Planck or Smoluchowski equation and is sometimes utilized as a model of classical Brownian motion.

$$\frac{\partial \rho(x,t)}{\partial t} = D_0 \frac{\partial^2 \rho(x,t)}{\partial x^2} \tag{3.1}$$

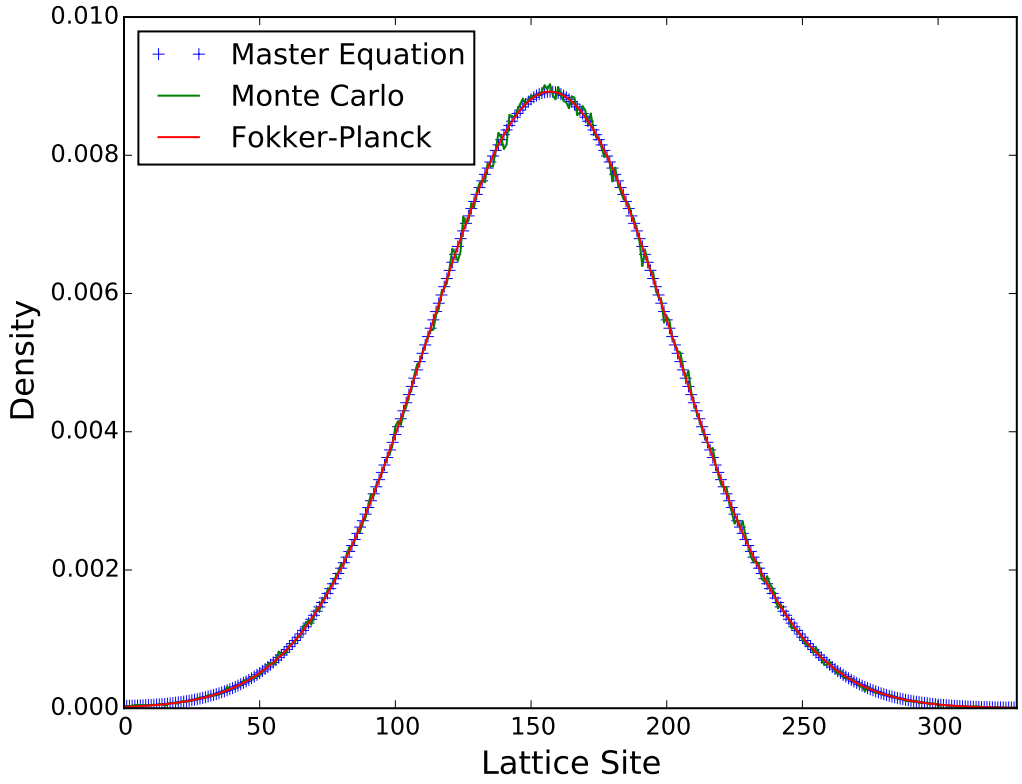

Figure 3.1: Simple 1D system with no internal semi-permeable boundaries. Simulation solutions plotted for ME and MC methods. Additionally, an exact solution to diffusion equation (Fokker-Planck) is plotted. Parameter specifications: 330 lattice sites, $D = 0.1$, $N = 8 \cdot 10^5$ particles in MC simulation, and density normalized.

Assuming that N particles start from the origin, Equation 3.1 has the solution:

$$\rho(x,t) = \frac{N}{\sqrt{4\pi D t}} e^{-\frac{x^2}{4Dt}} \tag{3.2}$$

A variant of Equation 3.2 was used to create the Fokker-Planck plot in Figure 3.1. The solution to 3.1 is not a solution to a boundary value problem. For example, it is possible to solve 3.1 for reflecting absolute boundary conditions: $\rho_x(0,t) = \rho_x(L,t) = 0$. It is even possible to solve it for 'repeating' boundary conditions that represent semi-permeable internal boundaries (Jessica Cervi's thesis); these specific problems were not explored and are not discussed further. However, it is comparatively easy

to obtain a solution to such a system with internal semi-permeable and absolute reflecting boundaries by utilizing MC and ME methods for the simulation of the system; Figure 3.2 shows such a solution.

With reference to Figure 3.1, note the good agreement between the ME and MC simulation solutions and analytical solution. The ME simulation solution and analytical solution are perfectly superimposed. The MC simulation shows characteristic statistical fluctuations that reflect the underlying 'random' movement of individual particles in the simulation. The relative magnitude of these fluctuations decreases with an increasing number of particles N according to $1/\sqrt{N}$.

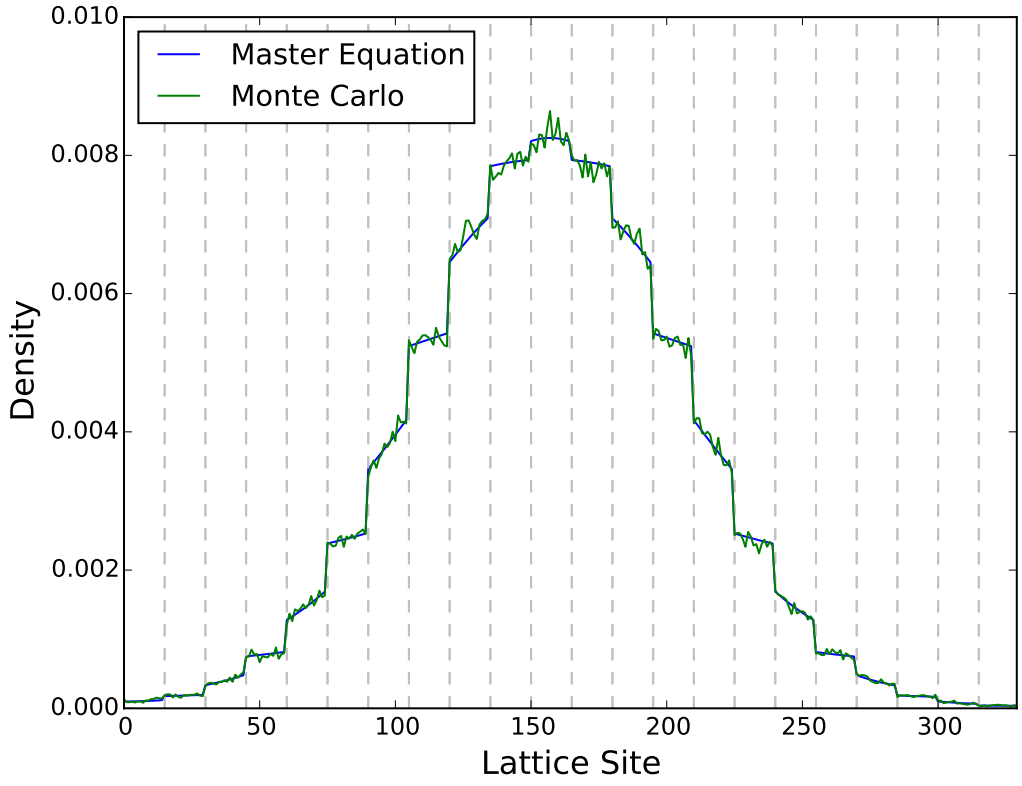

Figure 3.2: 1D heterogeneous system with internal semi-permeable boundaries. Simulation solutions plotted for ME and MC methods. Parameter specifications: 330 lattice sites, 15 lattice sites per cellular or extracellular region, $D_i = 0.05$, $D_e = 0.2$, and $P_{i \to e} = 0.05$. $N = 5 \cdot 10^5$ particles in the MC simulation and density normalized. Vertical dashed lines show semi-permeable boundary positions.

Statistical fluctuations in the MC simulation solution are more visible in Figure 3.2. The ME simulation was orders of magnitude faster in reaching completion and does not show any fluctuations since the density distribution is evolved in time under the assumption that there are *very* many particles at each lattice site. It is expected that in the limit of an infinite number of particles, the MC solution converges to the ME solution. Comparisons to analytical or numerical solutions of the Fokker-Planck equation were not made but doing so may be of interest in the future.

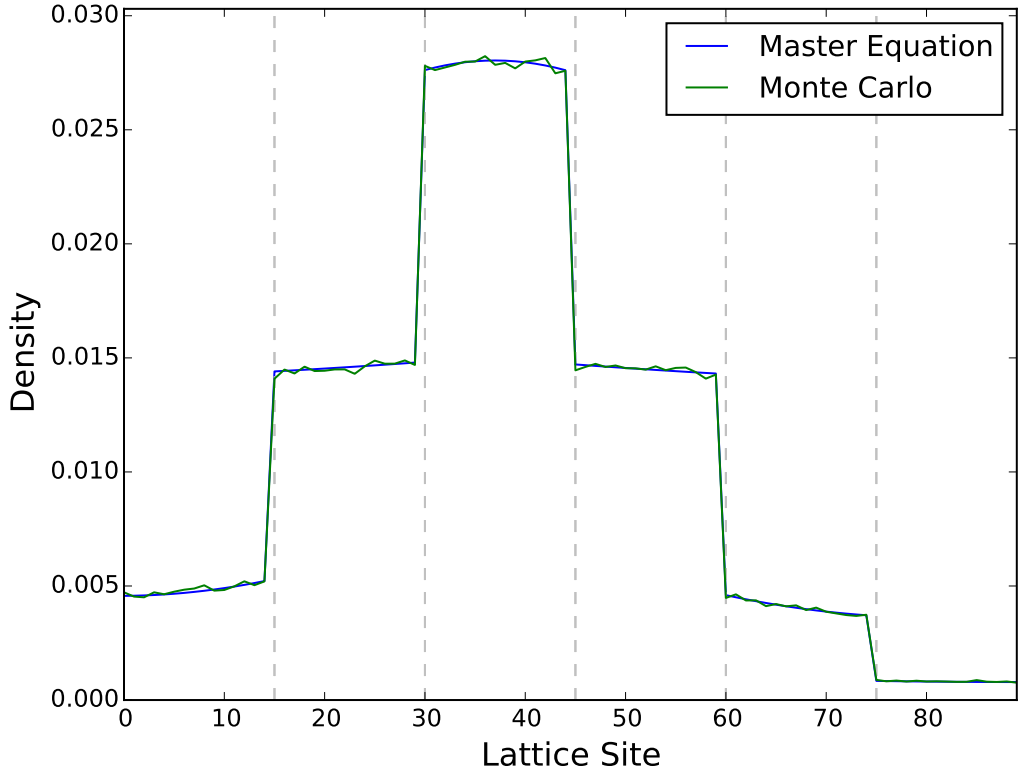

Figure 3.3: 1D heterogeneous system with internal semi-permeable boundaries. Simulation solutions plotted for ME and MC methods. Parameter specifications: 90 lattice sites, 15 lattice sites per cellular or extracellular region, $D_i = 0.05$, $D_e = 0.2$, and $P_{i \to e} = 0.01$. $N = 8 \cdot 10^5$ particles in the MC simulation and density normalized. Vertical dashed lines show semi-permeable boundary positions.

Interesting to note in Figure 3.2 and 3.3, the magnitude of the fluctuations in the MC solution appear larger at higher densities and smaller at lower densities. In Figure 3.2, extracellular regions with 4-times larger diffusivity equilibrate faster than the cellular regions; this is visible as 'flat' versus 'sloped' density distributions. Figure 3.3 shows behaviour at the absolute reflecting boundaries.

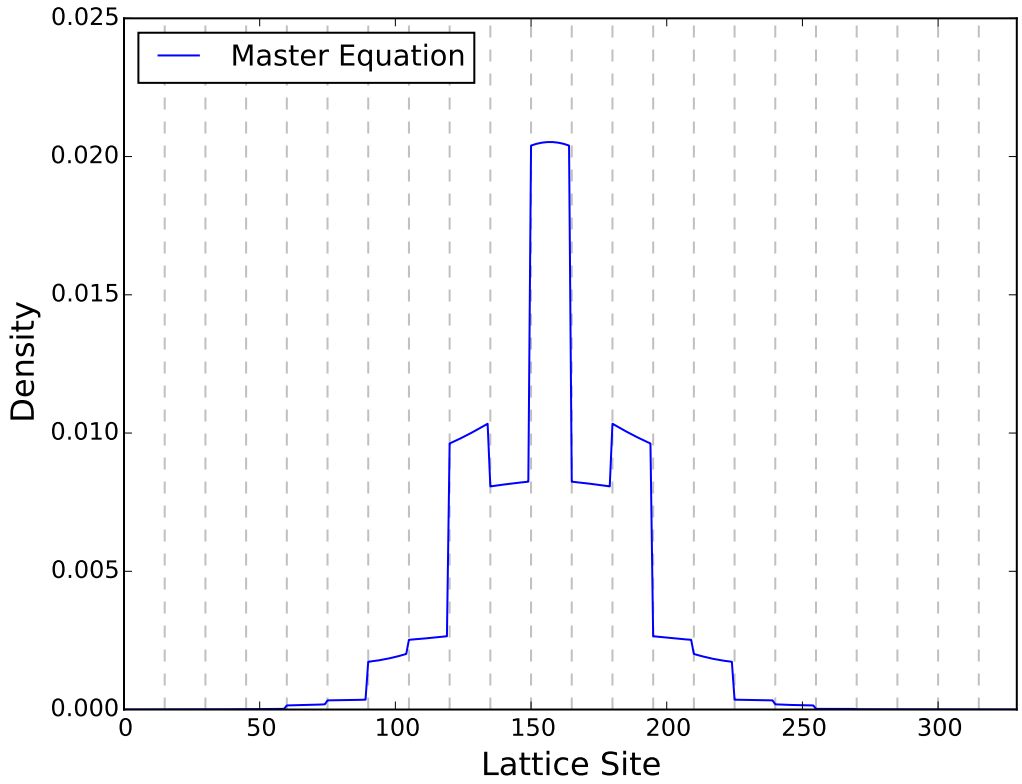

Figure 3.4: 1D heterogeneous system with internal semi-permeable boundaries. Non-physical density distribution simulated by violating the semi-permeable boundary condition (sometimes known as the isothermal boundary condition). Parameter specifications: 330 lattice sites, 15 lattice sites per cellular or extracellular region, $D_i = 0.05$, $D_e = 0.2$, and $P_{i\to e} = 0.01$ and $P_{e\to i} = 0.005$. Correctly chosen, $P_{e\to i} = 0.0025$. Vertical dashed lines show semi-permeable boundary positions.

Figure 3.4 shows the necessity of having coupled transition probabilities for the semi-permeable boundaries. The distribution in the long-time limit does not approach a uniform distribution, as would be expected for any system with passive semi-permeable boundaries and reflecting absolute boundaries. In the long-time, the density grows in certain cells and shrinks in others, similar to what might be expected if the semi-permeable boundaries behaved in an active-selective manner.

Section 3.1.1 explores the effects of changing the semi-permeable boundary transition probability while maintaining region diffusivities constant. The second and last section 3.1.2 explores the effects of changing the ratio of the cellular and extracellular (C/EC) diffusivities while maintaining the semi-permeable boundary transition probability constant. In both sections and for all simulations, the size of the unit cell was constant, and C/EC regions were of the same dimensions.

3.1.1 Boundary Transition Probabilities

The total transition probability is the product of two probabilities; the probability that a particle steps towards a boundary and the transition probability. The transition probability $P_{i\to e}$ ("pie" in figure) is specified but the corresponding probability $P_{e\to i}$ can be easily calculated since the probabilities are coupled. For each plot, a different transition probability tested while all other parameters were held constant.

In Figure 3.5, the slope is clearly not unity for all time, for most of the plots, indicating the presence of anomalous diffusion. With decreasing transition probability, the magnitude of deviation from steady diffusion increases. Interestingly, for the largest transition probability simulated ($P_{i\to e} = 0.150$), the magnitude of deviation from steady diffusion is very small. It may be possible that for large transition probabilities, as long as the semi-permeable boundary transition condition is respected, approximately steady diffusion occurs for all time. In the long-time, the diffusion process becomes steady again for all transition probabilities tested.

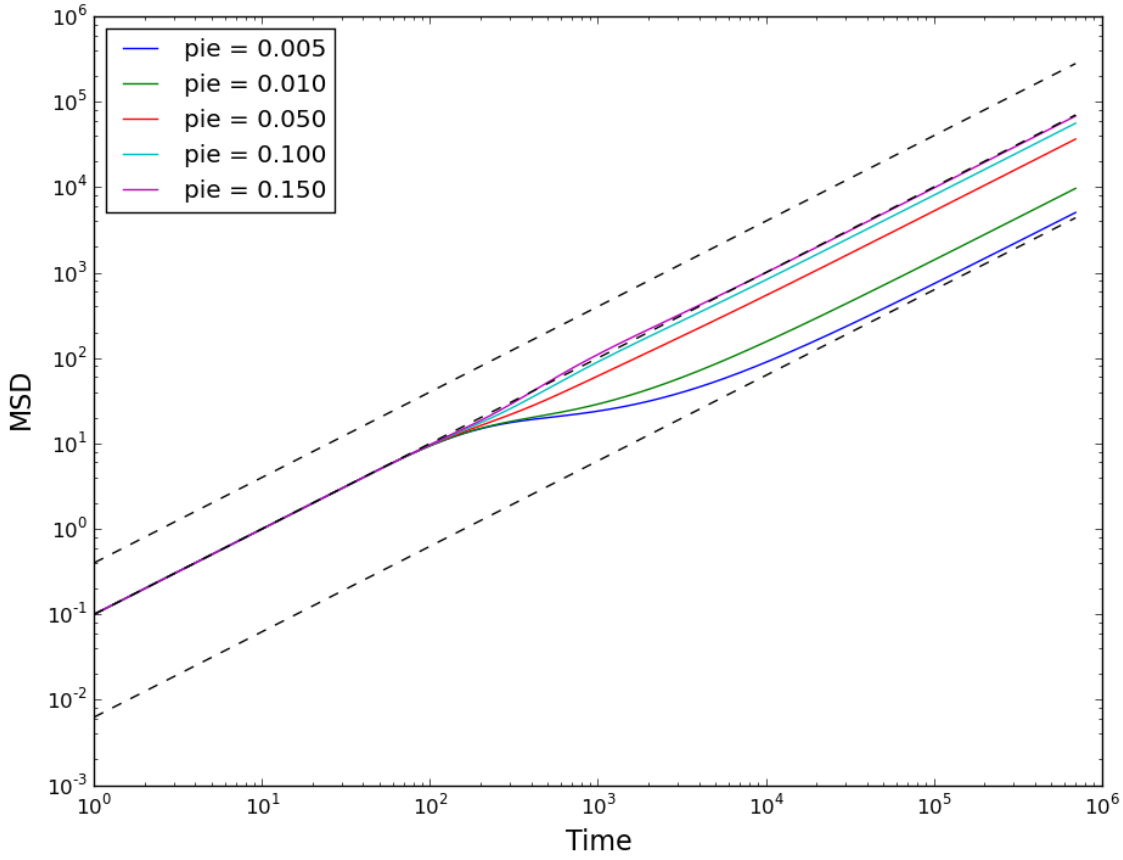

Figure 3.5: MSD versus time for 1D heterogeneous system. Parameter specifications: 3330 lattice sites, 15 lattice sites per cellular or extracellular region, $D_i = 0.05$, $D_e = 0.2$, and simulation time is $7 \cdot 10^5$ time steps. $D = 0.2$ for top dashed line, $D = 0.05$ for middle dashed line, and $D = 0.5 \cdot (P_{i \to e} + P_{e \to i})$ for the bottom dashed line (an average of the transition probabilities).

In Figure 3.6, the extent of the anomalous diffusion is clear in the $\beta(t)$ versus t top figure. For all transition probabilities, steady diffusion occurs from the start of the simulation to some time where particles meet the semi-permeable boundary; this occurs at the same time for all simulations since C/EC diffusivity was constant. Both the magnitude of sub-diffusive behaviour and length of time before reaching steady diffusion, increase with decreasing transition probability. Super-diffusive behaviour appears only for two transition probabilities; it might be interesting to find the threshold transition probability that results in super-diffusive behaviour.

In the bottom figure, the effective diffusivity may approach an average of the

boundary transition probabilities, at least for transition probabilities much smaller than C/EC diffusivities. This is shown for $P_{i\to e} = 0.150$ and is observed for the other transition probabilities as well; however, this 'average approach' sometimes under- or over-estimates the effective diffusivity obtained in the simulations and does not work well for transition probabilities approaching C/EC diffusivities, which may indicate dependence on regional diffusivities.

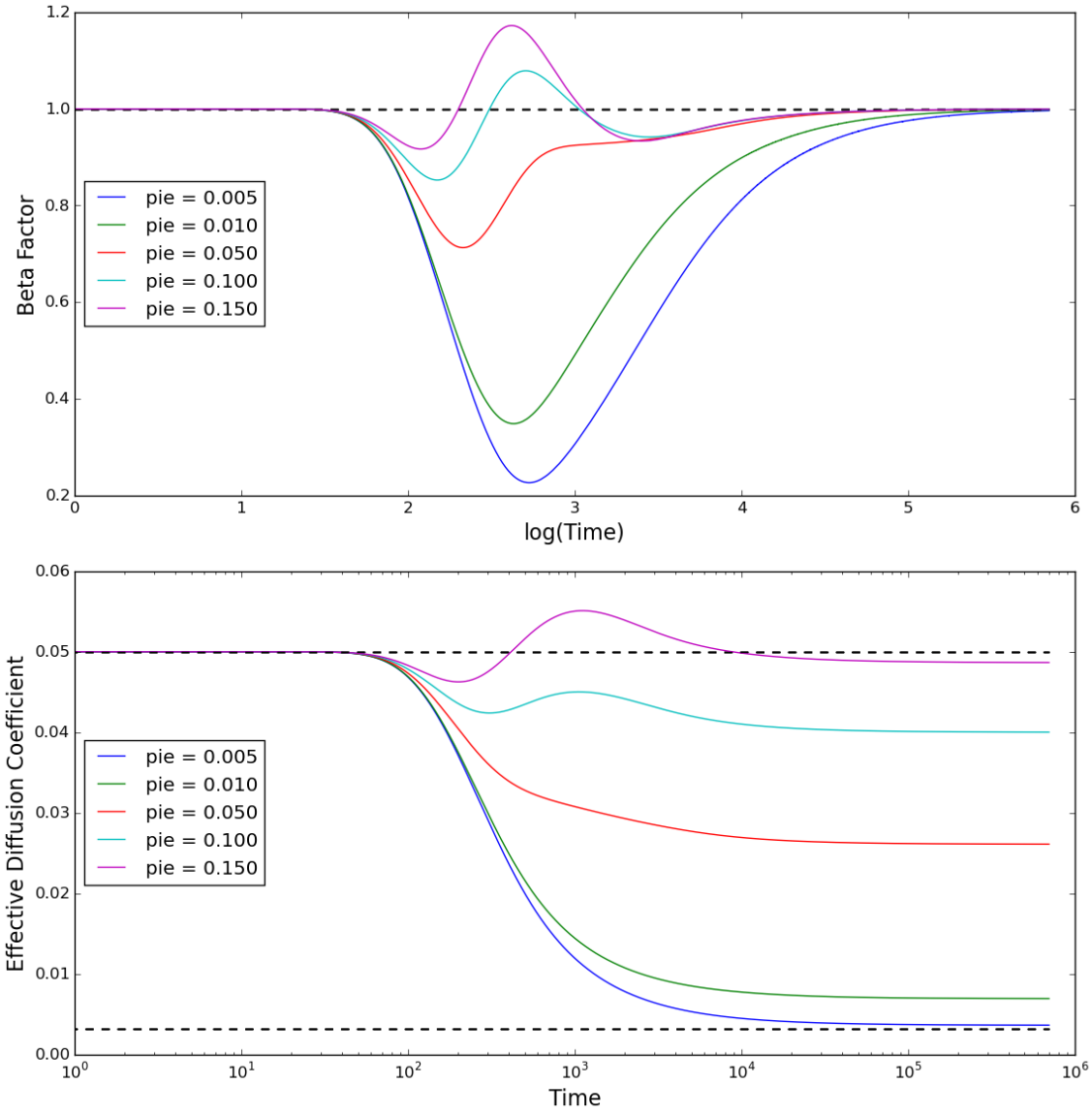

Figure 3.6: $\beta(t)$ versus log(time) and D_{eff} versus time for 1D heterogeneous system. Parameter specifications: 3330 lattice sites, 15 lattice sites per cellular or extracellular region, $D_i = 0.05$, $D_e = 0.2$, and simulation time is $7 \cdot 10^5$ time steps. In the lower figure, $D = 0.05$ for the upper dashed line and $D = 0.5 \cdot (P_{i \to e} + P_{e \to i})$ for the lower dashed line (an average of the transition probabilities).

3.1.2 Cellular and Extracellular Diffusivities

For each plot, the ratio of cellular to extracellular diffusivities (indicated as "pi/pe" on the figures), while all other parameters were held constant. More specifically, the cellular diffusivity was varied while the extracellular diffusivity was constant.

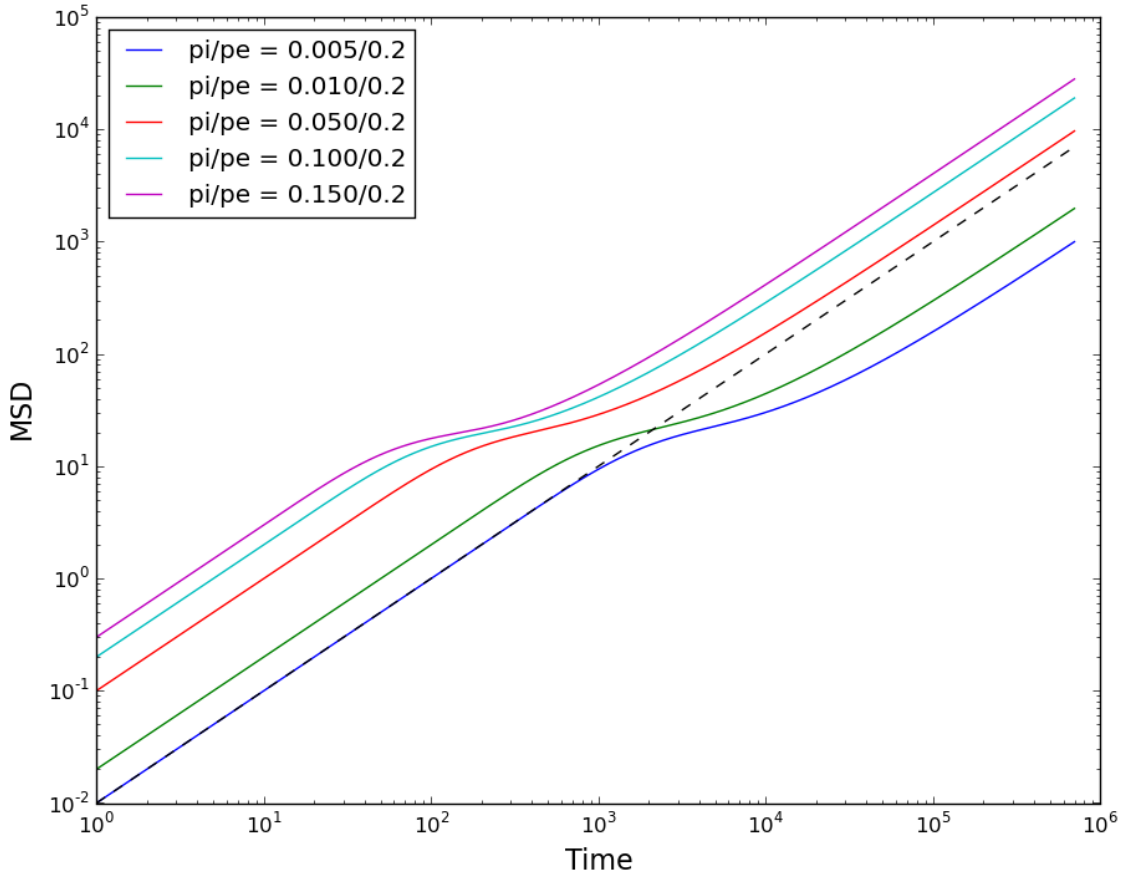

Figure 3.7: MSD versus time for 1D heterogeneous system. Parameter specifications: 3330 lattice sites, 15 lattice sites per cellular or extracellular region, $P_{i \to e} = 0.01$, and simulation time is $7 \cdot 10^5$ time steps. $D = 0.005$ for the dashed line.

In Figure 3.7, anomalous diffusion is observed for all diffusivity ratios and in particular, no super-diffusive behaviour occurs. This last point is clearly evident in Figure 3.8; none of the ratios tested result in $\beta > 1$ for any time. The displacement of the peak of the curves in time is due to the varying cellular diffusivities tested. The larger the diffusivity of the region in which the particles start, the quicker the particles

reach the semi-permeable boundary and sub-diffusive behaviour occurs. Interestingly, the magnitude in the deviation from steady diffusion is approximately the same for all C/EC diffusivity ratios.

The effective diffusion in the long-time is non-trivial; it does not seem to approach some derivable value. It likely depends on the C/EC diffusivities and transition probabilities but the relationship is not obvious. All that can be said for now is qualitative; for every C/EC diffusivity ratio tested, the effective diffusivity in the long time is less than the starting region diffusivity and the larger the starting diffusivity, the greater the difference from the long-time effective diffusivity. For ratios close to unity and transition probabilities very small, the effective diffusion coefficient may approach the average of the transition probabilities but this cannot be said with certainty. Further testing is needed.

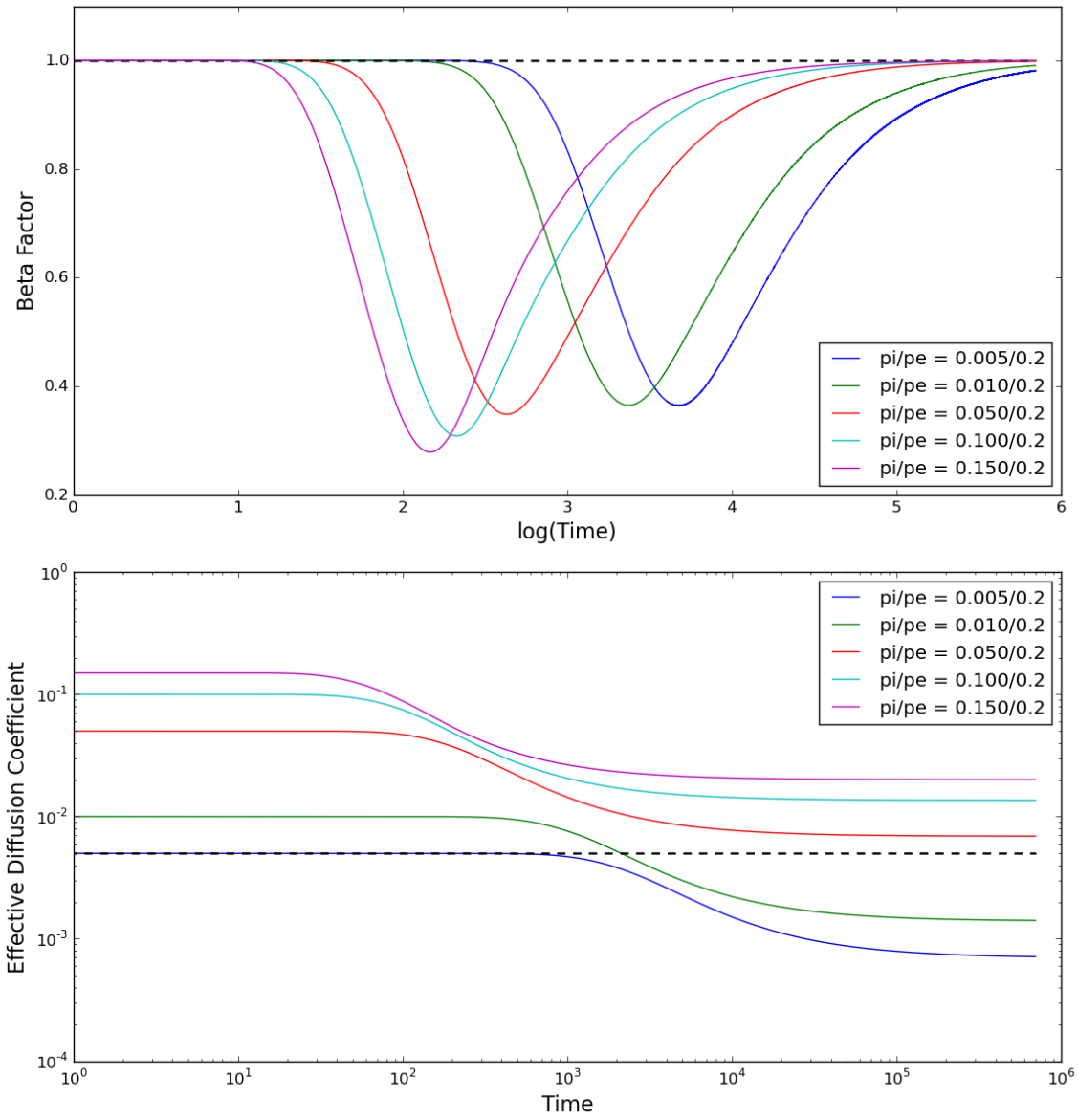

Figure 3.8: $\beta(t)$ versus log(time) and D_{eff} versus time for 1D heterogeneous system. Parameter specifications: 3330 lattice sites, 15 lattice sites per cellular or extracellular region, $P_{i\to e} = 0.01$, and simulation time is $7 \cdot 10^5$ time steps. In the lower figure, $D = 0.005$ for the dashed line.

3.2 2D Systems

The analysis of 2D systems proceeded in the same manner as for 1D systems, except with the addition of another variable for testing: extracellular channel width. Section 3.2.1 explores the effects of changing the semi-permeable boundary transition probability while maintaining C/EC diffusivities and channel width, constant. The second section 3.2.2 explores the effects of changing the ratio of the C/EC diffusivities while maintaining the semi-permeable boundary transition probabilities and channel width, constant. The third and final section 3.2.3 explores the effects of changing the width of the extracellular channel in $\hat{y}$ while maintaining the ratio of C/EC diffusivities and semi-permeable boundary transition probabilities, constant.

The 2D system is divided into two halves, upper and lower. The upper halve consists of alternating cellular and extracellular regions of the same and square geometry; the dimensions of these regions were the same for every simulation. The lower halve consists of a single extracellular channel.

Due to the computational time required to simulate using MC, all simulations used for analysis were ME simulations and because of the additional physical dimension, more particles are needed in the MC simulation to obtain smoother distributions with smaller fluctuations. Figure 3.9 and 3.10 show 'heat maps' of the 2D density distribution at the same time step, for comparison. Figure 3.11 shows diffusion in a larger system where particles have not reached the absolute boundaries and Figure 3.12 shows a barely visible non-physical density distribution, created by purposely violating the "iso-thermal" semi-permeable boundary condition.

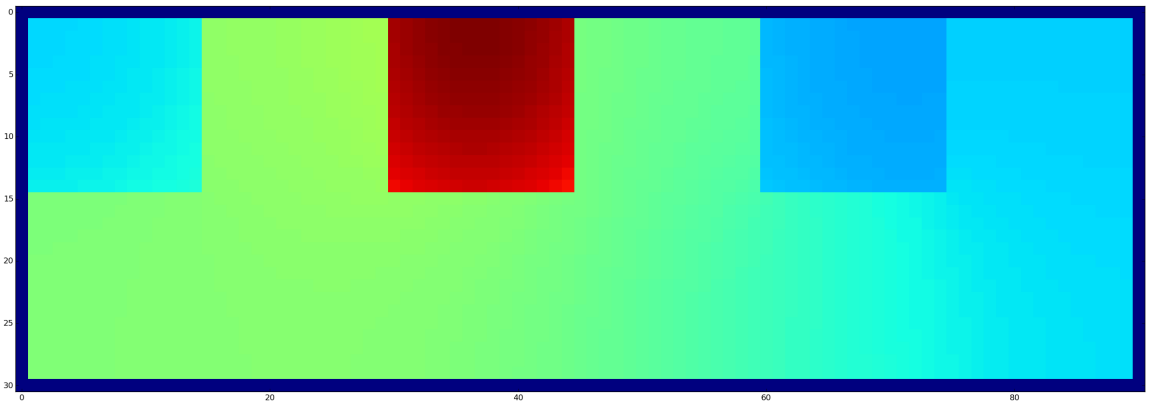

Figure 3.9: Master equation simulation of diffusion in a 2D heterogeneous system. Parameter specifications: 90 lattice sites in $\hat{x}$ and 30 lattice sites in $\hat{y}$, (15×15) lattice sites per cellular or extracellular region, $D_i = 0.05$, $D_e = 0.2$, and $P_{i \to e} = 0.025$. Semi-permeable boundaries are clearly visible.

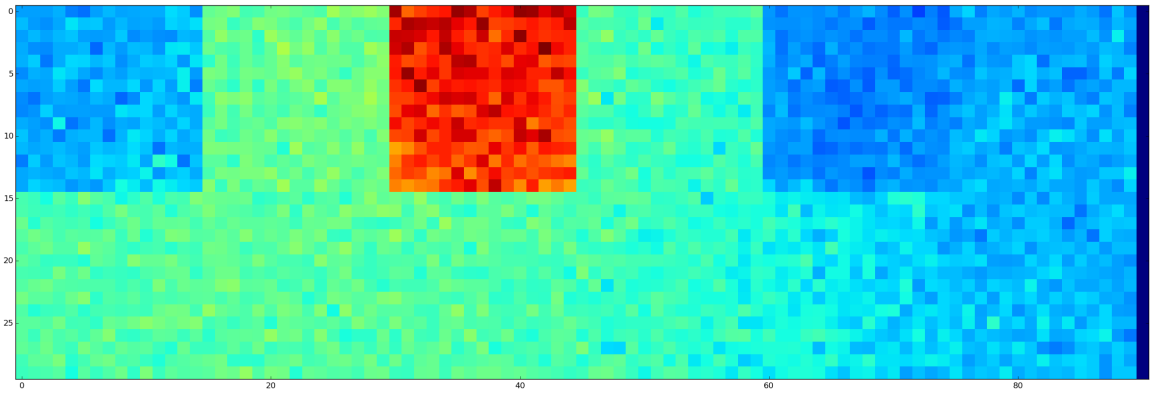

Figure 3.10: Monte Carlo simulation of diffusion in a 2D heterogeneous system. Parameter specifications: 90 lattice sites in $\hat{x}$ and 30 lattice sites in $\hat{y}$, (15×15) lattice sites per cellular or extracellular region, $D_i = 0.05$, $D_e = 0.2$, and $P_{i \to e} = 0.025$, $N = 5 \cdot 10^5$ particles used.

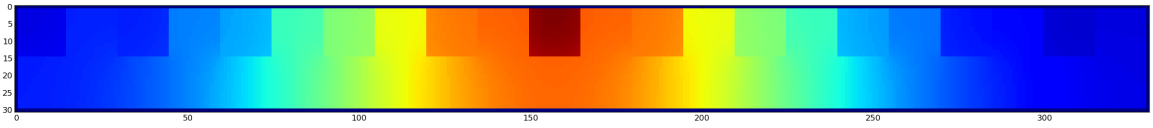

Figure 3.11: Master equation simulation of diffusion in a larger 2D heterogeneous system. Parameter specifications: 90 lattice sites in $\hat{x}$ and 330 lattice sites in $\hat{y}$, (15×15) lattice sites per cellular or extracellular region, $D_i = 0.05$, $D_e = 0.2$, and $P_{i \to e} = 0.025$, $N = 5 \cdot 10^5$ particles used.

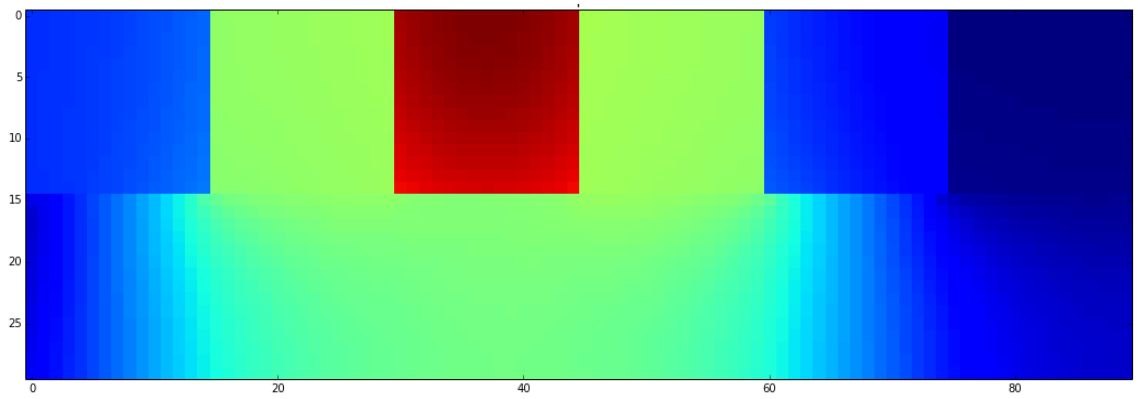

Figure 3.12: Master equation simulation of diffusion in 2D heterogeneous system. Non-physical density distribution simulated by violating the semi-permeable boundary condition. Note the slightly visible 'boundary' edges separating the upper extracellular region from lower extracellular channel. Errors may be less perceivable than in the 1D simulations and will likely not be visible until many time steps have elapsed and the system is very small.

3.2.1 Boundary Transition Probabilities

For all transition probabilities tested ("pie" in figures), anomalous diffusion behaviour is present. Inspection of the MSD versus time plots in Figure 3.13, shows initial sub-diffusive behaviour caused by particles meeting semi-permeable boundary of the starting region, followed by super-diffusive behaviour as particles exit their initial enclosure and reach the high-diffusivity extracellular region. Note that a single MC simulation was run with the same parameters as the corresponding ME simulation. The two are in good agreement but D_{eff} calculated from the MC simulation is slightly smaller than calculated from the ME simulation, beyond a time where most particles have left the starting region. This discrepancy may by due to the finite number of particles used and the statistical error introduced by low particle densities.

In Figure 3.14, similar to the 1D case, the magnitude of the deviation from steady diffusion decreases with increasing transition probability, except now there is also super-diffusive behaviour present due to the extracellular channel. Observe the diffusive behaviour in the case of $P_{i\to e} = 0.150$, there is a temporary plateau where the magnitude of super-diffusive behaviour is constant for some interval of time. Inter-

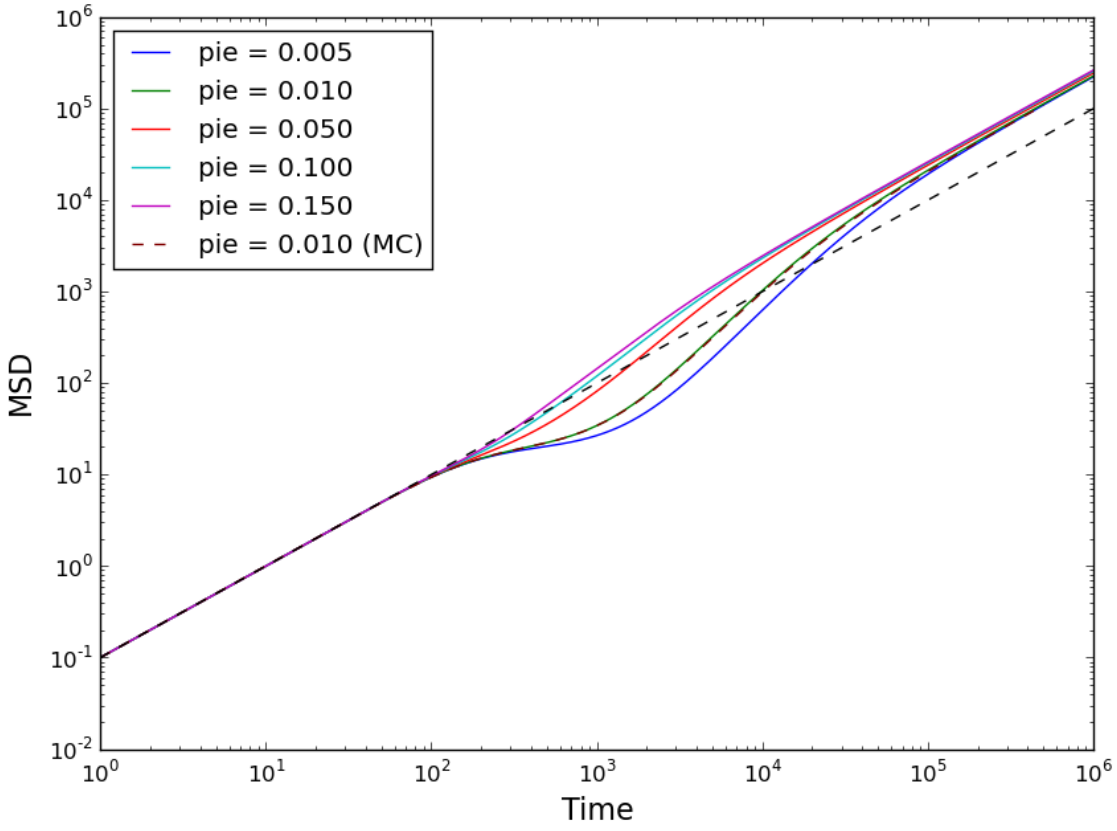

Figure 3.13: MSD versus time for 2D heterogeneous system. Parameter specifications: 3630 lattice sites, 15 lattice site channel width, (15×15) lattice sites per cellular or extracellular region, $D_i = 0.05$, $D_e = 0.2$, and simulation time is 10^6 time steps. $D = 0.05$ for the dashed line.

estingly, in the β versus $\log(t)$ plot, the time difference between the maximum and minimum of each plot increases with decreasing transition probability. Essentially, the time spent in anomalous diffusion by a system increases with decreasing transition probability.

The effective diffusivity in the long-time is non-trivial and its dependence on the boundary transition probabilities, C/EC diffusivity ratios, and channel geometry is not obvious.

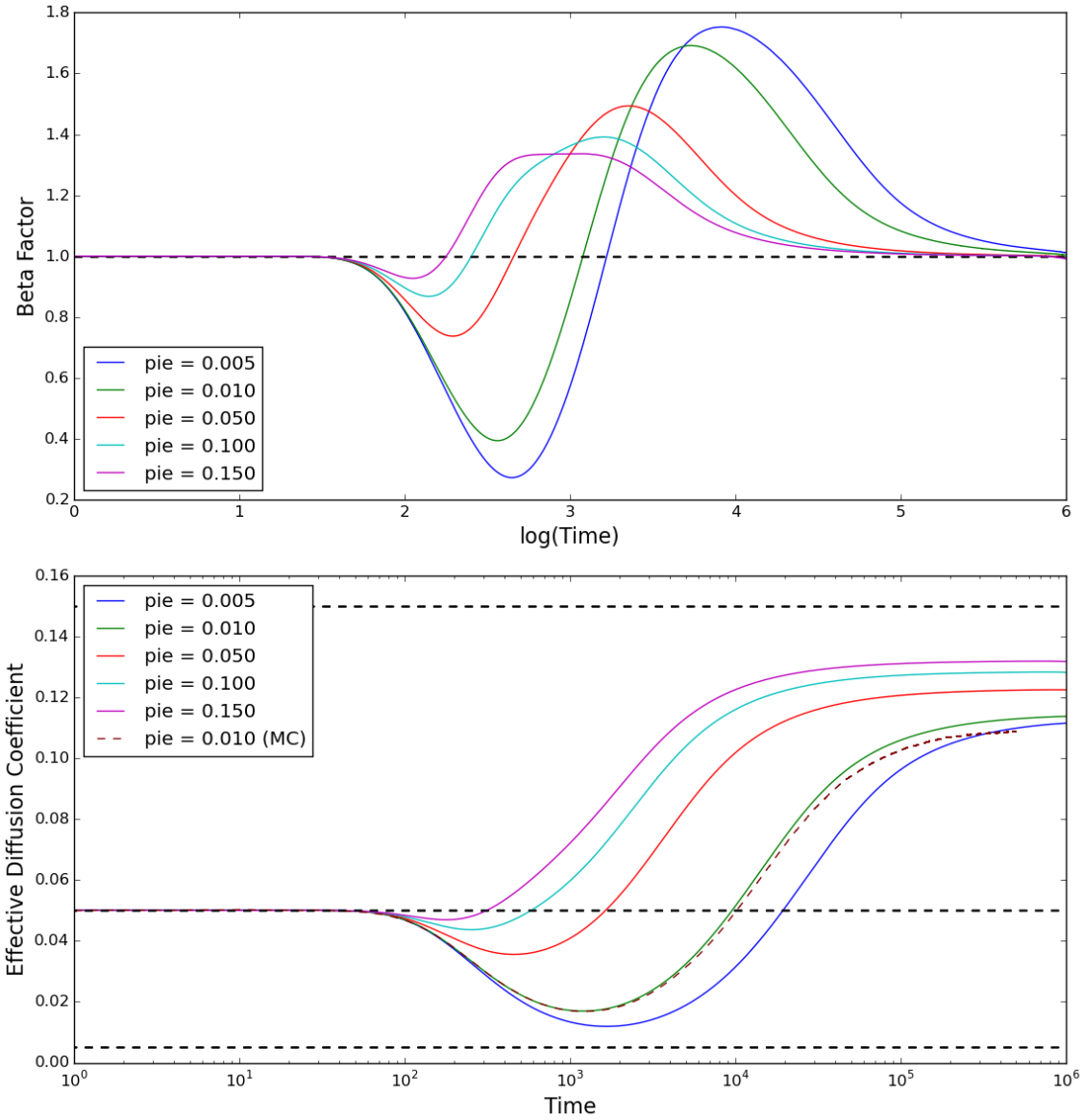

Figure 3.14: $\beta(t)$ versus log(time) and D_{eff} versus time for 2D heterogeneous system. Parameter specifications: 3630 lattice sites, 15 lattice site channel width, (15×15) lattice sites per cellular or extracellular region, $D_i = 0.05$, $D_e = 0.2$, and simulation time is 10^6 time steps. In the lower figure, $D = 0.15$ for the top dashed line and $D = 0.05$ for the middle dashed line, and $D = 0.005$ for the bottom dashed line.

3.2.2 Cellular and Extracellular Diffusivities

For all ratios of C/EC diffusivity tested ("pi/pe" in figures), it appears that regardless of the diffusivity of the starting region, the long-time effective diffusion coefficients are nearly the same.

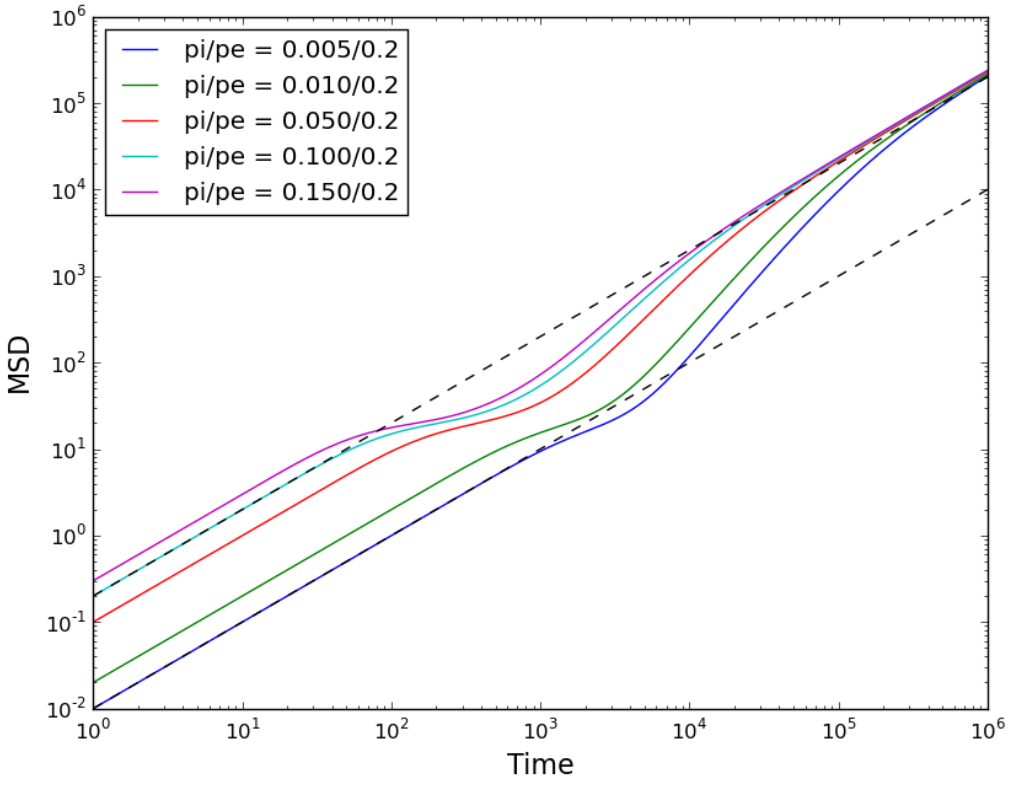

Figure 3.15: MSD versus time for 2D heterogeneous system. Parameter specifications: 3030 lattice sites, 15 lattice site channel width, (15×15) lattice sites per cellular or extracellular region, $D_e = 0.2$, $P_{i \to e} = 0.01$, and simulation time is 10^6 time steps. $D = 0.1$ for the upper dashed line and $D = 0.005$ for the lower dashed line.

Compared to the 1D simulations where only sub-diffusive behaviour was observed, sub- and super-diffusive behaviour is observed for all C/EC ratios tested, in the 2D simulations. The displacement in the minimum of each plot in Figure 3.16 is characteristic of different diffusivities in the particle's starting region.

The long-time effective diffusion coefficients appear to converge to the same value, but it is unclear how this value depends on the parameters tested and it is unknown

how changing other parameters might affect this long-time value. It might be interesting to test how the long-time effective diffusion coefficient depends on specific values of D_i and D_e, while maintaining the ratio of these values constant.

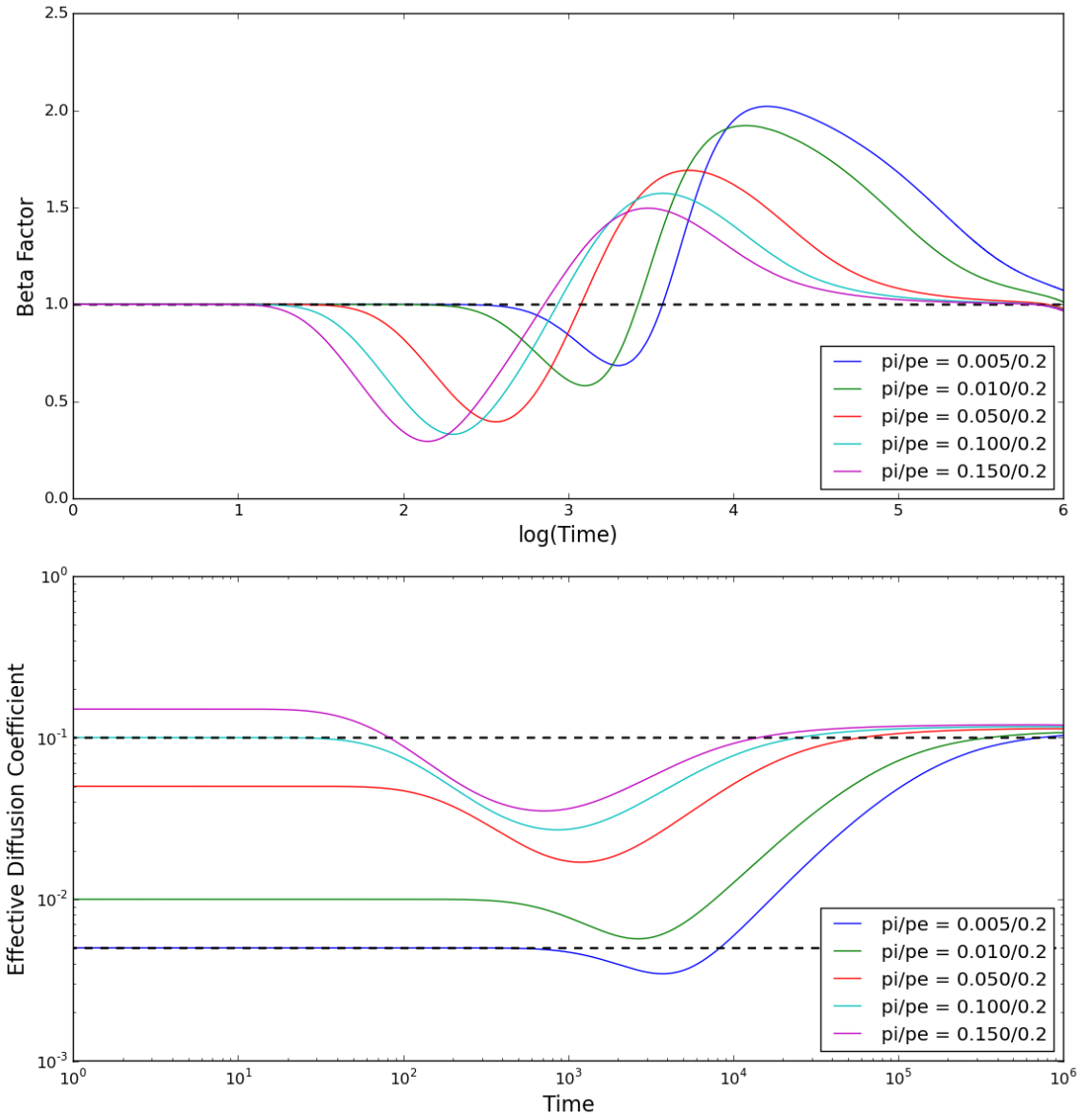

Figure 3.16: $\beta(t)$ versus log(time) and D_{eff} versus time for 2D heterogeneous system. Parameter specifications: 3030 lattice sites, 15 lattice site channel width, (15×15) lattice sites per cellular or extracellular region, $D_e = 0.2$, $P_{i \to e} = 0.01$, and simulation time is 10^6 time steps. In the lower figure, $D = 0.1$ for the upper dashed line and $D = 0.005$ for the lower dashed line.

3.2.3 Extracellular Channel Widths

The extracellular channel may be used as a 'conduit' for particles and it is possible that once leaving the initial enclosure, a particle may not interact with a semi-permeable boundary. Therefore, how the dimensions of this channel affect diffusive behaviour and the long-time effective diffusion coefficient are of interest. The standard channel width for all other simulations was 15 lattice units. A channel width of 0 lattice units was also tested in order to simulate a pseudo-1D system.

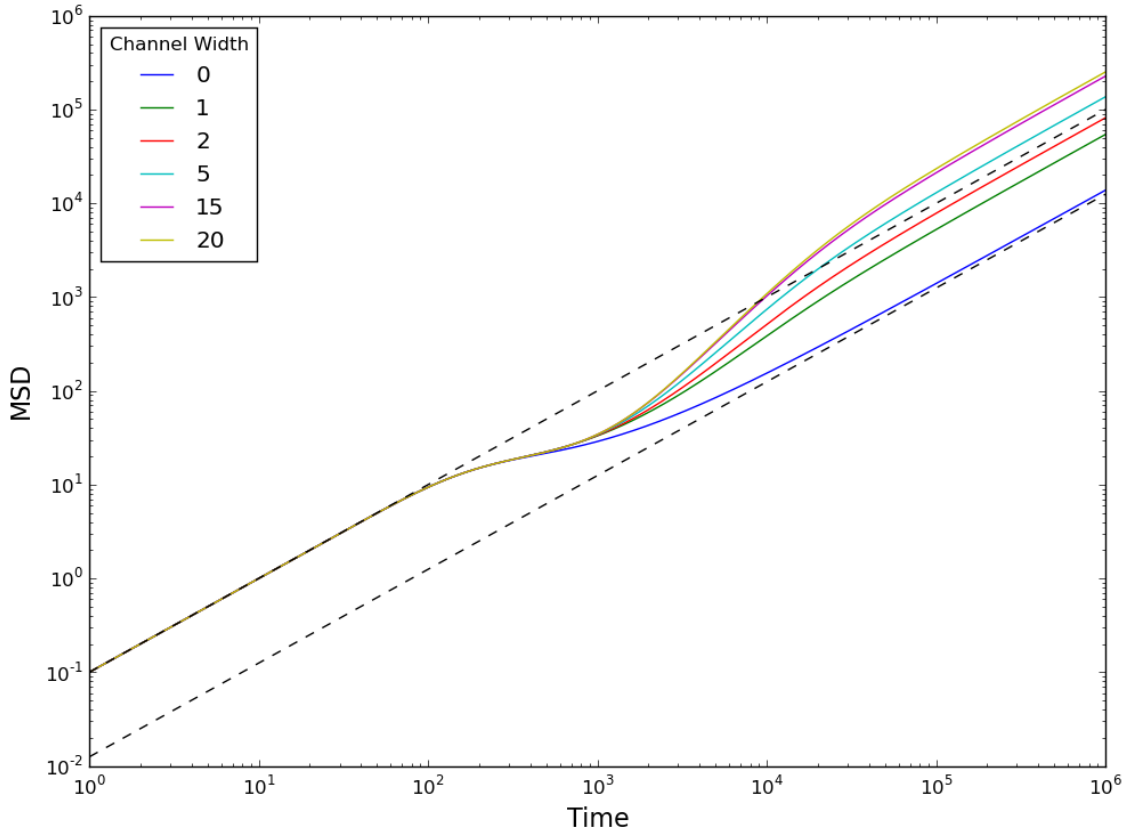

Figure 3.17: MSD versus time for 2D heterogeneous system. Parameter specifications: 3030 lattice sites, (15×15) lattice sites per cellular or extracellular region, $D_i = 0.05$, $D_e = 0.2$, $P_{i \to e} = 0.01$, and simulation time is 10^6 time steps.

Similar to the 1D system with the same diffusivity and transition probability parameters, only sub-diffusive behaviour occurred in the 2D system with no extracellular channel (refer to Figure 3.5 and 3.6). Observe in Figure 3.18, the addition of even a

single (1) lattice site as an extracellular channel results in super-diffusive behaviour. It appears the change in diffusion behaviour becomes less dramatic with increasing channel width. Larger channel widths need to be tested to verify this and identify how β might depend on channel width.

It is not certain how the long-time effective diffusivity depends on the channel width and other parameters. What can be said is that increasing the width of the channel makes more of the highly diffusive extracellular space available for the particles, therefore it is expected that larger channel widths result in greater long-time effective diffusivities (up to a certain limit: the extracellular diffusivity).

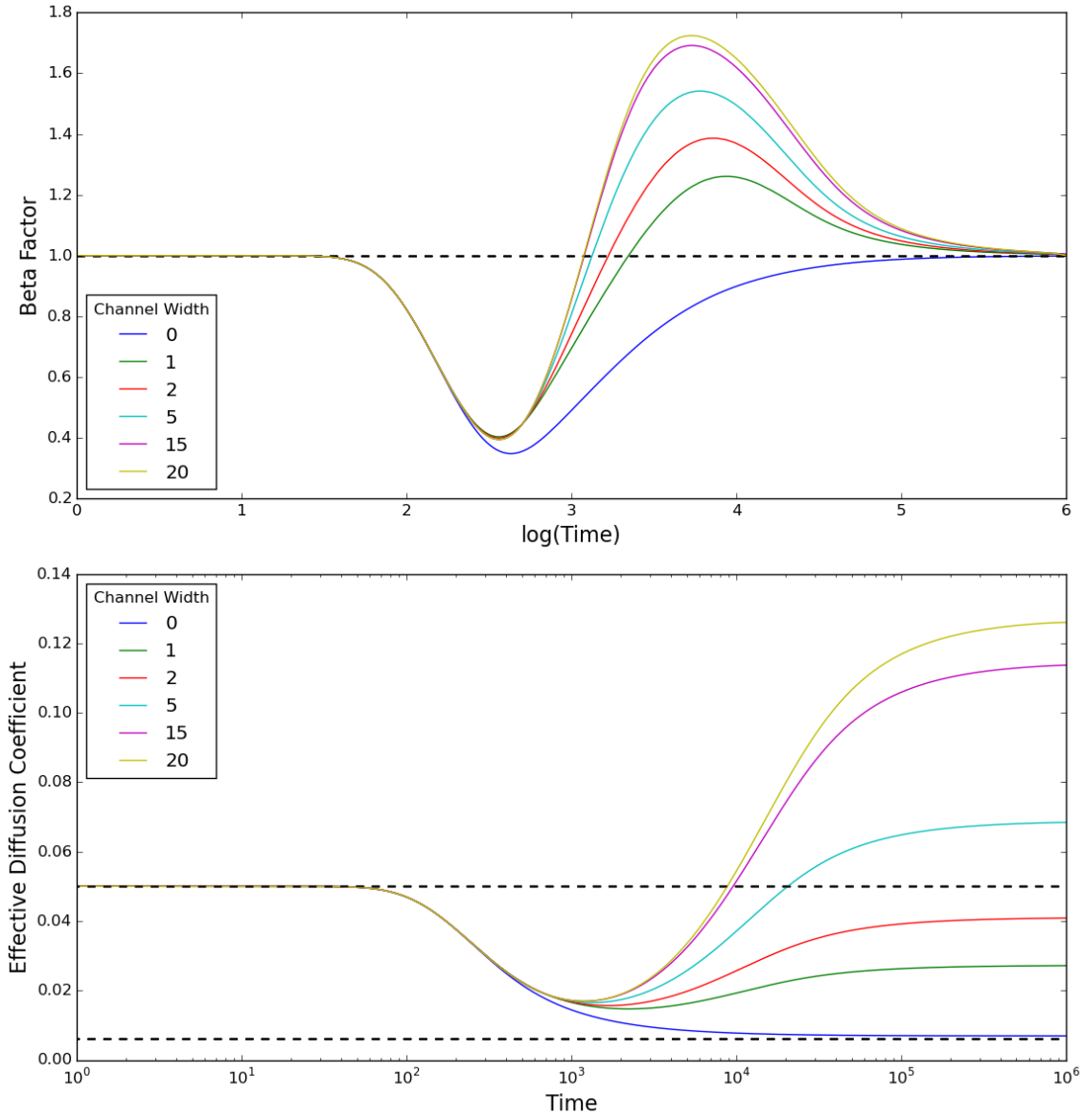

Figure 3.18: $\beta(t)$ versus log(time) and D_{eff} versus time for 2D heterogeneous system. Parameter specifications: 3030 lattice sites, (15×15) lattice sites per cellular or extracellular region, $D_i = 0.05$, $D_e = 0.2$, $P_{i \to e} = 0.01$, and simulation time is 10^6 time steps. In the lower figure, $D = 0.05$ for the upper dashed line and $D = 0.5 \cdot (P_{i \to e} + P_{e \to i})$ for the lower dashed line (an average of the transition probabilities, similar to the 1D case).

4. FUTURE WORK AND CONCLUSION

May just put this into the results section near the end as conclusions and future work.

REFERENCES

Navarro, J.F., Frenk, C.S., & White, S.D.M. 1995, MNRAS, 275, 720

Campbell, N.A., Reece, J.B., et al. 2008. Biology. 8th ed. Pearson Benjamin Cummings.

Patton K.T., Thibodeau G.A.. 2013, 8th ed. Elsevier.

One and a Half Century of Diffusion: Fick, Einstein, Before and Beyond. Jean Philibert, diffusion-fundamentals.org **4** (2006) 6, pp 6.1-6.19.

A. APPENDIX

This is just an example of an appendix.